Water Research 232 (2023) 119686

Contents lists available at ScienceDirect

Water Research

journal homepage: www.elsevier.com/locate/watres

Inactivation of the waterborne marine pathogen *Vibrio alginolyticus* by photo-chemical processes driven by UV-A, UV-B, or UV-C LED combined with H_2O_2 or HSO_5^-

Javier Moreno-Andrés *, Miguel Tierno-Galán, Leonardo Romero-Martínez, Asunción Acevedo-Merino, Enrique Nebot

Department of Environmental Technologies, Faculty of Marine and Environmental Sciences. INMAR-Marine Research Institute, CEIMAR- International Campus of Excellence of the Sea. University of Cadiz, Spain

ARTICLE INFO

Keywords:
Ultraviolet
LED
Marine bacteria
Aquaculture
Ballast water
Reactivation

ABSTRACT

Ultraviolet (UV) radiation is a well-implemented process for water disinfection. The development of emergent UV sources, such as light-emitting diodes (LEDs), has afforded new possibilities for advanced oxidation processes. The emission wavelength is considered to be an important factor for photo-chemical processes in terms of both biological damage and energetic efficiency, as the inactivation mechanisms and mode-of-action may differ according to the wavelength that is applied. In addition, these processes merit exploration for inactivating emerging pathogens, such as marine vibrios, that are important bacteria to control in maritime activities. The main goal of this study was to compare the disinfection efficacy of several UV-LED driven processes with different modes of action. First, the effect of UV-LEDs was assessed at different UV ranges (UV-A, UV-B, or UV-C). Second, the possible enhancement of a combination with hydrogen peroxide (H_2O_2) or peroxymonosulfate salt (HSO_5^-) was investigated under two different application strategies, i.e. simultaneous or sequential. The results obtained indicate a high sensitivity of *Vibrio alginolyticus* to UV radiation, especially under UV-B (k_{obs} = 0.24 cm^2/mJ) and UV-C (k_{obs} = 1.47 cm^2/mJ) irradiation. The highest inactivation rate constants were obtained for UV/HSO_5^- (k_{obs} (cm^2/mJ)=0.0007 (UV-A); 0.39 (UV-B); 1.79 (UV-C)) with respect to UV/H_2O_2 (k_{obs} (cm^2/mJ)= 0.0006 (UV-A); 0.26 (UV-B); and 1.54 (UV-C)) processes, however, regrowth was avoided only with UV/H_2O_2. Additionally, the disinfection enhancement caused by a chemical addition was more evident in the order UV-A > UV-B > UV-C. By applying H_2O_2 (10 mg/L) or HSO_5^- (2.5 mg/L) in a sequential mode before the UV, negligible effects were obtained in comparison with the simultaneous application. Finally, promising electrical energy per order (EE_O) values were obtained as follows: UV/HSO_5^- (EE_O (kWh/m^3)=1.68 (UV-A); 0.20 (UV-B); 0.04 (UV-C)) and UV/H_2O_2 (EE_O (kWh/m^3)=2.15 (UV-A); 0.32 (UV-B); 0.04 (UV-C)), demonstrating the potential of UV-LEDs for disinfection in particular activities such as the aquaculture industry or maritime transport.

1. Introduction

Ultraviolet disinfection is a conventional option for inactivating a variety of waterborne organisms (Bolton and Cotton, 2008; Song et al., 2016). Its effectiveness for abating a wide variety of detrimental microorganisms has opened its field of application to other particular activities such as marine aquaculture (Summerfelt, 2003) or ballast water treatment (Hess-Erga et al., 2019).

UV technology has traditionally been employed at a monochromatic (λ = 254 nm) or polychromatic (200–400 nm) emission with low- or medium-pressure mercury lamps. Nonetheless, in the search for UV light sources that are more sustainable, the light-emitting diodes (LEDs) have demonstrated effectiveness as a promising alternative to mercury lamps (Chen et al., 2017; Umar et al., 2019). Additionally, UV LEDs are a mercury-free UV source that has gained significance according to the Minamata Convention on Mercury (UNEP, 2019). The development of LEDs as a UV source has also afforded new possibilities for advanced water treatment processes in terms of photocatalytic or photochemical processes. This is due to its ability to obtain a tailored emission spectrum along with the greater freedom for reactor design because of the

* Corresponding author.
E-mail address: javier.moreno@uca.es (J. Moreno-Andrés).

https://doi.org/10.1016/j.watres.2023.119686
Received 26 September 2022; Received in revised form 24 January 2023; Accepted 29 January 2023
Available online 31 January 2023

distribution of multiple LEDs along the photo-reactor (Jeon et al., 2022; Jo and Tayade, 2014; Martín-Sómer et al., 2018; Romero-Martínez et al., 2022).

Photocatalytic methods have shown promising results in disinfection (Levchuk et al., 2019; Moreno-Andrés et al., 2020b). However, their efficiency can be significantly affected by the relatively high salinity of the marine environment that lessens disinfection effectiveness (Levchuk et al., 2019; Moreno-Andrés et al., 2017), and thus raises concerns about the viability of this type of treatment in such a complex water matrix (Porcar-Santos et al., 2020). On the other hand, photochemical processes (UV/H_2O_2, UV/persulfate, UV/O_3, or UV/chlorine) have revealed promising results for water treatment over the last years (Miklos et al., 2018). UV/H_2O_2 processes have been widely studied in terms of disinfection, specifically under UV-C or solar irradiation (Feng et al., 2020; Giannakis et al., 2016; Moreno-Andrés et al., 2016). The use of persulfate salts (specifically, peroxymonosulfate salt as HSO_5^-) has also shown encouraging results for bacteria inactivation, as it is able to achieve inactivation levels similar to those of UV/H_2O_2 (Berruti et al., 2021; Guerra-Rodríguez et al., 2022; Moreno-Andrés et al., 2019; Qi et al., 2020). However, although H_2O_2 or HSO_5^- are favourable oxidizing chemicals in photo-assisted processes, their implementation still presents some concerns in terms of environmental sustainability, being the electricity a relevant parameter (Pesqueira et al., 2022). Accordingly, as UV-LEDs are expected to increase in electrical efficiency, they would be a promising technology for the water-energy nexus (Jeon et al., 2022; Martín-Sómer et al., 2023).

The inactivation mechanisms and mode-of-action of UV/H_2O_2 or UV/HSO_5^- may differ according to the wavelength that is applied. In this regard, intracellular mechanisms might prevail over extracellular mechanisms as the emission wavelength increases (Berruti et al., 2022; Feng et al., 2020; Giannakis et al., 2022). Accordingly, the emission wavelength is considered to be an important factor for ensuring a proper evaluation of photo-chemical processes in terms of both biological damage and energetic efficiency. In parallel, there is a lack of an integrative and comparative study of specific emission wavelengths in the three main UV ranges: UV-A (315–400 nm), UV-B (280–315 nm), and UV-C (200–280 nm).

The majority of the research in this area has been focused on an urban wastewater matrix and less attention has been paid to other relevant water matrices that requires disinfection, such as seawater (Aguilar et al., 2018; Hess-Erga et al., 2019; Qi et al., 2020). In addition, the bacterial indicators selected to address the different inactivation processes are usually the typical indicators related to fecal pollution such as *Escherichia coli* (Qi et al., 2020; Rubio et al., 2015; Zhang et al., 2022). Nonetheless, the survival of *E. coli* is negatively correlated with salinity (Giannakis et al., 2014) as seawater ecosystems are a hostile environment for fecal bacteria (Belkin et al., 2005). Thus, the regrowth of specific marine bacteria becomes relevant after disinfection processes (Hess-Erga et al., 2010; Moreno-Andrés et al., 2018; Wennberg et al., 2013). However, the inactivation of marine bacteria together with the underlying bacterial inactivation mechanisms and the influence of inorganic ions in seawater has not often been examined (Wang et al., 2021).

Vibrio species (Family *Vibrionaceae*) are ubiquitously present in estuarine and marine environments (Baker-Austin et al., 2017; Reen et al., 2006). In fact, the genus Vibrio is considered as a bacterial indicator in some international policies such as the Regulation D-2 of the Ballast Water Management Convention (IMO, 2004). Although many species of the genus Vibrio are not pathogenic, there are four species of relevance that have emerged as opportunistic human pathogens and emergent pathogens of aquaculture species (Baker-Austin et al., 2017): *V. cholerae; V. vulnificus; V. parahaemolyticus*, and *V. alginolyticus*. In this study, *V. alginolyticus* was selected as the target bacterium for inactivation experiments. It is an overlooked bacterium that is recognized as an emerging human pathogen but also associated with disease in a wide variety of fish, crustaceans, or bivalves (Baker-Austin et al., 2017; Reen et al., 2006). In addition, their occurrence in ballast waters (Khandeparker et al., 2020) where they might exhibit resistance to beta-lactam antibiotics (Ng et al., 2018), along with their relationship with harmful algal blooms (Bellés-Garulera et al., 2016), make it an important bacterium to control due to the risk of pathogen emergence from environmental sources. Although a number previous studies have considered the UV-mediated inactivation of the Vibrio species (Table S1), the specific UV inactivation performance of *V. alginolyticus* has been less studied. In this regard, photochemical processes used against the marine pathogen *V. alginolyticus* are worth exploring.

To do so, this study compared the disinfection efficacy of several UV-LED driven processes with different modes of action. Firstly, the effect of UV-LEDs in different UV ranges were assessed: UV-A (λ_{max} = 365 nm); UV-B (λ_{max} = 300 nm) or UV-C (λ_{max} = 275 nm). Secondly, the possible enhancement of a combination of these UV-LEDs with hydrogen peroxide (H_2O_2) or peroxymonosulfate salt (HSO_5^-) was investigated under two different strategies of application, i.e. simultaneously or in a sequential mode. Finally, in order to provide a wide-ranging idea of the viability of these processes, regrowth and considerations about the energy efficiency are also presented. In this regard, the wavelength effect as well as the optimization of UV-Dose for marine water disinfection are the main motivation of this study.

2. Material and methods

2.1. Microbiological procedures

The bacterium *V. alginolyticus* (CECT 521T; ATCC 17749) was selected as the target microorganism for the different inactivation tests. *V. alginolyticus,* typical in marine environments, is considered as an emergent pathogen as previously indicated. A pure strain (isolated from spoiled *Trachurus trachurus* causing food poisoning) was acquired from the Spanish Type Culture Collection (CECT, University of Valencia).

The pure bacterial strain from a lyophilized culture was reactivated and preserved in water: glycerol (50:50) at −35 °C. For each set of experiments, the reactivation of each vial was performed from a frozen stock that was also used in previous studies (Moreno-Andrés et al., 2020a). Briefly, each vial was resuspended in Marine Broth (PanReac AppliChem) and incubated aerobically at 30 °C for 24 h. After two cycles, the subculture was considered metabolically active, thus it was subjected to a centrifugation process at 3000 rpm for ten minutes, which allowed the separation of the marine broth (supernatant) from the cells (in the pellet form). Bacterial cells were then transferred to actual seawater thereby obtaining an inoculum ready for experimentation. It was subsequently diluted to create a working solution for the experiments that ensured an initial concentration of approximately 10^6 CFU·mL^{-1}.

Bacterial survival after treatment was assessed with standard plate counts (in triplicate) with Thiosulfate Citrate Bile Salts Sucrose (TCBS Agar, VWR Chemicals). After the incubation period (30 °C, 24 h), colonies were counted. In order to ensure a measurable number of CFUs (15–150), tenfold dilutions were plated. The detection limit was 10 CFU·mL^{-1}. Analyses were performed in triplicate using a variation coefficient of less than 30% as the acceptance criteria.

2.2. UV-LED reactor

A collimated beam reactor equipped with UV-LED technology (Photolab LED275–0.01/300–0.03/365–1cb; APRIA Systems S.L., Spain) was used for the experimentation. The photoreactor was equipped with three UV-LED devices emitting at three different wavelengths distinguished by UV-A (1200 mW): 365 – 370 nm, λ_{max} = 365 nm; UV-B (32 mW): 295–305 nm, λ_{max} = 300 nm, or UV-C (10.5 mW): 265–285 nm, λ_{max} = 275 nm.

The photoreactor contains a collimator tube with a collimator lens with a diameter of 5.08 cm and focal length of 6 cm. The treatment was

applied to samples in Petri dishes with a diameter of 55 mm and capacity for 20 mL of target water. A magnetic stirrer with a volume of 0.25 mL was added to the Petri dish for continuous stirring throughout irradiation. The sample surface was at 12.2 cm from the UV light source. The irradiance was measured with a radiometer (HD 2102.1, Delta OHM) that was equipped with a probe according to the specific emission wavelength (Delta OHM LP471 – UVA, UVB or UVBC). The measured irradiance at the sample surface was determined as 60 ± 2.55 $W{\cdot}m^{-2}$ (UV-A), 1.36 ± 0.07 $W{\cdot}m^{-2}$ (UV-B), and 0.39 ± 0.04 $W{\cdot}m^{-2}$ (UV-C), with Petri factors of 0.945 (UV-A), 0.957 (UV-B), and 0.995 (UV-C).

The UV-dose of each UV-LED can be calculated as the product of exposure time and UV light intensity, including several factors that affect it in the collimated beam (Bolton and Linden, 2003). Thus, the germicidal irradiance was obtained based on the reactor morphometry, measured irradiance, and water transmittance at the maximum wavelength emission of each UV-LED (Text S1).

2.3. Experimental approach

Experimentation was conducted in ground saltwater that was collected from the Campus of Puerto Real of the University of Cádiz, Spain (pH = 7.65, conductivity = 48.9 $mS{\cdot}cm^{-1}$, salinity = 35.8 and TOC = 1.98 mg $C{\cdot}L^{-1}$). The raw water was filtered through 0.45 μm and sterilized in an autoclave at 121 °C in order to avoid particulate material as well as lowering the viral or bacterial load in the actual water.

Different inactivation tests were performed with a similar experimental set-up of those in previous studies (Moreno-Andrés et al., 2016). Briefly, they were arranged with water inoculated with *V. alginolyticus* to the collimated beam reactor. The treatment was applied to samples in Petri dishes with a continuous stirring throughout irradiation. Sampling was fixed at regular exposure times which implies different UV-doses.

Firstly, single UV tests were performed by evaluating the disinfection efficacy of the three different UV-LEDs wavelengths. Secondly, photochemical tests were conducted by combining hydrogen peroxide (H_2O_2, 30%, ultrapure, Scharlau) or peroxymonosulfate (HSO_5^-, obtained from Oxone©, Sigma-Aldrich; $KHSO_5 \cdot 0.5KHSO_4 \cdot 0.5K_2SO_4$,) with UV irradiation. To address the effect of combined processes, three experimental phases were defined:

I Effect of H_2O_2 or HSO_5^- in darkness. Based on previous optimization studies (Feng et al., 2020; Moreno-Andrés et al., 2016, 2019; Rodríguez-Chueca et al., 2019), 10 mg of $H_2O_2{\cdot}L^{-1}$ (0.29 mM) and 2.5–10 mg of $HSO_5^-{\cdot}L^{-1}$ (0.008 – 0.034 mM) were selected as appropriate reagent concentrations for assessing photo-disinfection processes.

II Simultaneous combination of UV/H_2O_2 or UV/HSO_5^-. The reagents were added in a single dosage and immediately exposed to UV radiation by fixing exposure times up to 60 min (UV-A) or 5 min (UV-B and UV-C) which implies maximum UV-Doses of 16.32 $J{\cdot}cm^{-2}$ (UV-A), 33.60 $mJ{\cdot}cm^{-2}$ (UV-B), and 8.40 $mJ{\cdot}cm^{-2}$ (UV-C).

III In a third set of experiments, the effect of combining oxidants with UV radiation was studied sequentially. For this, H_2O_2 or HSO_5^- was added first, and the mixture was kept in darkness under continuous agitation for 30 min in order to provide a sufficient amount of time for the reagent to penetrate the cell and initiate intracellular oxidation (Feng et al., 2020; Zhang et al., 2014). After this time, irradiation began, and the sampling procedure was done in the same way as that in point ii).

In order to obtain a comprehensive scenario of the disinfection process, the regrowth of bacteria was monitored for each disinfection method. After the inactivation assays (assuring a 3 Log-Removal Values), water samples were stored in sterile flasks in darkness at an ambient temperature (20 ± 2 °C) for 24 h. In these experiments, the residual oxidant was not neutralized to evaluate the possible effects after the treatment. Due to the scope of the present work, photoreactivation experiences were not considered given the unlikelihood of the treated water being exposed to light after treatment, especially in the ballast water situation.

The H_2O_2 concentration was measured with a colorimetric method with titanium (IV) oxysulfate ($TiOSO_4$, 1.9–2.1%, Fluka) at 410 nm (DIN 38,409 H15). A similar colorimetric method with KI was attempted for the measurement of HSO_5^-, however, it was not possible due to the low concentrations used which were very close to the detection limit (1.35 $mg{\cdot}L^{-1}$) of this procedure (Wacławek et al., 2015). In addition, the molar absorption coefficient of each reagent was estimated by obtaining the UV–Vis spectra. All of these procedures were measured with a Jenway 7315 spectrophotometer.

2.4. Data treatment

The response of the *V. alginolyticus* to the different photo-chemical processes was obtained by plotting the logarithmic reduction of the survival microorganisms (Log (N/N_0)) versus exposure time or UV-Dose. The experimental points were fitted according to the well-established mathematical model of pseudo-first order (Eq. 1) for which "k_{obs}" is the kinetic rate constant of inactivation that was obtained by means of exposure time (t, s^{-1}) or UV-dose ($cm^2{\cdot}mJ^{-1}$).

$$N = N_0\ e^{-kobs\ t\ or\ UV\ Dose} \tag{1}$$

A GinaFiT tool was employed to fit the inactivation results on the kinetic model (Geeraerd et al., 2005). Accordingly, the kinetic rate constant (± Standard Error) was obtained. Additionally, the different inactivation profiles were analyzed statistically to check for significant differences between the slopes of the inactivation profiles (Further ANOVA for variables in the order fitted) using Statgraphics© Centurion XVIII. Additionally, in order to quantitatively assess the combination of the UV/H_2O_2 or UV/HSO_5 system, the synergy of the combined processes (S, dimensionless) was quantified according to Eq. (2) for which a positive value is representative of the synergistic effect (Dewil et al., 2017).

$$S = \frac{k_{combined} - \sum_1^n k_{individual}}{k_{combined}} \tag{2}$$

The percentage of regrowth was determined according to the Eq. (3) where N_r is the viable bacteria concentration of reactivated samples (after 24 h), N is the viable bacteria concentration in samples measured immediately after the UV irradiation, and N_0 is the initial bacterial concentration (Lindenauer and Darby, 1994).

$$Regrowth\ (\%) = 100 \cdot \frac{N_r - N}{N_0 - N} \tag{3}$$

Finally, the electrical energy per order, EE/O (kWh/m^3), was obtained as the amount of electrical energy required (per cubic meter) to reduce the bacterial concentration by an order of magnitude. EE/O estimations have been successfully applied to assess the performance of different UV disinfection systems with either UV-LEDs or low pressure mercury lamps as UV-sources (Beck et al., 2017; Li et al., 2019). The EE/O values were calculated according to Eq. (4) (Sharpless and Linden, 2005) that is based on the experimental set-up (A: irradiated surface area in cm^2; V: sample volume in liters; and WF: water factor (Bolton and Linden, 2003)), the experimental results obtained (k_{obs}, inactivation rate constant referred to the UV-dose, $cm^2{\cdot}mJ^{-1}$), and the wall-plug efficiency (C) of each specific UV-LED (provided by the manufacturer). The factor $3.6{\cdot}10^6$ was used to convert between hours to seconds, mW to kW, and L to m^3.

$$EE_O = \frac{A}{3.6{\cdot}10^6 \cdot V \cdot k_{obs} \cdot C \cdot WF} \tag{4}$$

3. Results and discussion

3.1. Inactivation by UV-LED in three emission range: UV-A, UV-B or UV-C

The first experiments were focused on the assessment of different UV-LEDs for the inactivation of *V. alginolyticus*. Time-response curves were obtained and depicted in Fig. 1 where different inactivation profiles were defined according to the emission wavelength, *i.e.,* UV-A, UV-B, or UV-C.

The inactivation profiles of *V. alginolyticus* differ according to the UV emission range exposures. For UV-A radiation, the inactivation is almost negligible (Fig. 1) whereas the inactivation rates notably improve with UV-B and UV-C exposures (Inset-Fig. 1). In order to quantify the inactivation rate according to the UV emission range, a log-linear decay was fitted to the experimental data, and kinetic constants (k_{obs}) were obtained (Table 1). Indeed, significant differences (p value < 0.01) between the slopes of the various inactivation profiles were determined for the distinct UV-LED exposures, including UV-B and UV-C. This indicates that the inactivation rate effectively increases according to the emission wavelength as UV-A < UV-B < UV-C.

These results can be explained by the fact that the sensitivity to ultraviolet light is wavelength-dependent (Pousty et al., 2021). Thus, the results obtained with UV-B exposures imply minor damage on *V. alginolyticus* than with the UV-C (42% less than the UV-C, according to the k_{obs}, s^{-1}). Although UV-C causes direct damage to cellular DNA, absorption by genetic material also occurs within the UV-B range, whereas the genetic material slightly absorbs within the UV-A range, producing mainly physiological alterations in the bacterial cells (Giannakis et al., 2022; Song et al., 2019). The main cell components affected by UV-A are involved in the metabolic cycle such as lipids, some proteins, and especially reactive oxygen species (ROS) scavengers such as catalases or superoxide dismutase (Feng et al., 2020; Giannakis et al., 2022). However, it has been demonstrated that these types of damage can effectively inactivate cells by triggering intracellular ROS formation (Giannakis et al., 2022) but at relatively higher UV-A doses (≈ 50–100 $J{\cdot}cm^{-2}$) that would require longer exposure times than those tested in this study (Giannakis et al., 2022; Song et al., 2019).

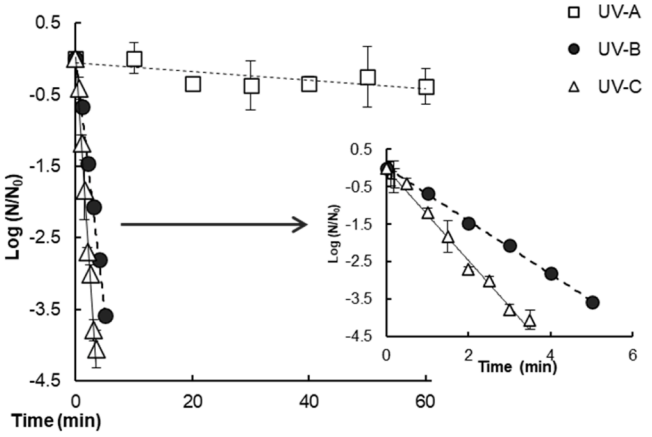

Fig. 1. Inactivation profiles of *V. alginolyticus* under UV irradiation at different wavelengths in terms of exposure time: UV-A (λ_{max} = 365 nm); UV-B (λ_{max} = 300 nm) or UV-C (λ_{max} = 275 nm). Symbols represent the mean of experimental points, and lines show a fit by Log-lineal model. **Specific data in terms of UV-Dose are explicitly reported on Table 1.*

In order to properly compare the results with literature, the inactivation rate constants in terms of the UV-Dose (k_{obs}, $cm^2{\cdot}mJ^{-1}$) together with that estimated for reaching a specific Log-Removal Value (LRV) were also calculated (Table 1). In this regard, the *V. alginolyticus* seems to be more sensitive to UV radiation than other typical bacterial indicators such as *E. coli* (Beck et al., 2017; Nyangaresi et al., 2018; Song et al., 2016). However, for other opportunistic bacteria like *Legionella pneumophila, Pseudomonas aeruginosa,* or *Vibrio parahaemolyticus*, the k_{max} (λ_{260}) is approximately 1 $cm^2{\cdot}mJ^{-1}$ with UV-Doses of 1.3–3.0 $mJ{\cdot}cm^{-2}$ per LRV (Oguma et al., 2019) which agrees with the results obtained in this study. In the case of a UV-B range (λ_{300}), similar kinetic rate constants were obtained when comparing with other types of bacteria (Oguma et al., 2019; Rattanakul and Oguma, 2018). Finally, with UV-A exposure, negligible inactivation effects were obtained. The maximum UV-A Dose applied in the present study was 18.1 $J{\cdot}cm^{-2}$ which resulted in a non-observable effect for *V. alginolyticus* inactivation. It also agrees with previous studies for which negligible effects were achieved for Vibrio species (Nakahashi et al., 2014) but also for other microorganisms including bacteria or viruses (Guerra-Rodríguez et al., 2022; Umar et al., 2019).

It is important to consider that some discrepancies in time-dose reciprocity might be obtained when scaling up the process in continuous reactors; this is possibly related to different UV damage mechanisms at longer wavelengths. In the specific case of *V. alginolyticus,* a time-intensity reciprocity was observed for a UV dose range between 0 and 7 mJ cm^{-2} within UV-C (λ_{max} = 275 nm) (Romero-Martínez et al., 2022). However, further studies are recommended to effectively address the biological damage that might not only be related to the UV Dose but also the exposure time, wavelength, and intensity (Pousty et al., 2021; Song et al., 2016).

3.2. Combination of UV-LED with H_2O_2 or HSO_5^-

3.2.1. UV/ H_2O_2 and UV/HSO_5^-

Firstly, the effect of different oxidants was tested in darkness. A slight bacterial mortality was quantified as 0.52 ± 0.41 LRV and 0.95 ± 0.39 LRV after the addition of H_2O_2 or HSO_5^- respectively, during 60 min of contact time. The specific results and discussion are detailed in the

Table 1
Kinetic parameters obtained related to the inactivation profiles of *V. alginolyticus* under different UV exposures (UV-A (λ_{max} = 365 nm); UV-B (λ_{max} = 300 nm) or UV-C (λ_{max} = 275 nm) and combined processes UV/H_2O_2 ([H_2O_2] =10 $mg{\cdot}L^{-1}$) or UV/HSO_5^- ([HSO_5^-]=2.5 $mg{\cdot}L^{-1}$). S.E.: standard error.

Treatment		k_{obs} ± SE (s^{-1})	k_{obs} ± SE ($cm^2{\cdot}mJ^{-1}$)		Estimated UV-Dose required for 1 or 4 LRV ($mJ{\cdot}cm^{-2}$)		Regrowth percentage after 24 h (%)
				R^2	D_1	D_4	
UV-A	UV	$2.30{\cdot}10^{-4} \pm 9.19{\cdot}10^{-5}$	$5{\cdot}10^{-5} \pm 2{\cdot}10^{-5}$	0.467	–	–	–[1]
	UV/H_2O_2	0.0023 ± 0.0006	$5.72{\cdot}10^{-4} \pm 1{\cdot}10^{-4}$	0.838	3598	–	0.0004
	UV/HSO_5^-	0.0035 ± 0.0007	$7.32{\cdot}10^{-4} \pm 1{\cdot}10^{-4}$	0.774	1992	7968	0.84
UV-B	UV	0.0273 ± 0.0004	0.244 ± 0.004	0.999	9.5	38.0	2.87
	UV/H_2O_2	0.028 ± 0.003	0.256 ± 0.026	0.941	7.8	31.1	−0.74
	UV/HSO_5^-	0.043 ± 0.005	0.393 ± 0.050	0.910	4.5	18.0	1.59
UV-C	UV	0.047 ± 0.002	1.474 ± 0.062	0.988	1.6	6.3	0.65
	UV/H_2O_2	0.050 ± 0.004	1.537 ± 0.144	0.949	1.3	5.0	−0.17
	UV/HSO_5^-	0.056 ± 0.003	1.793 ± 0.135	0.962	1.0	4.2	0.005

[1] It should be noted that the regrowth tests were not carried out for single UV-A due to the low inactivation rate that was obtained (See Section 3.1).

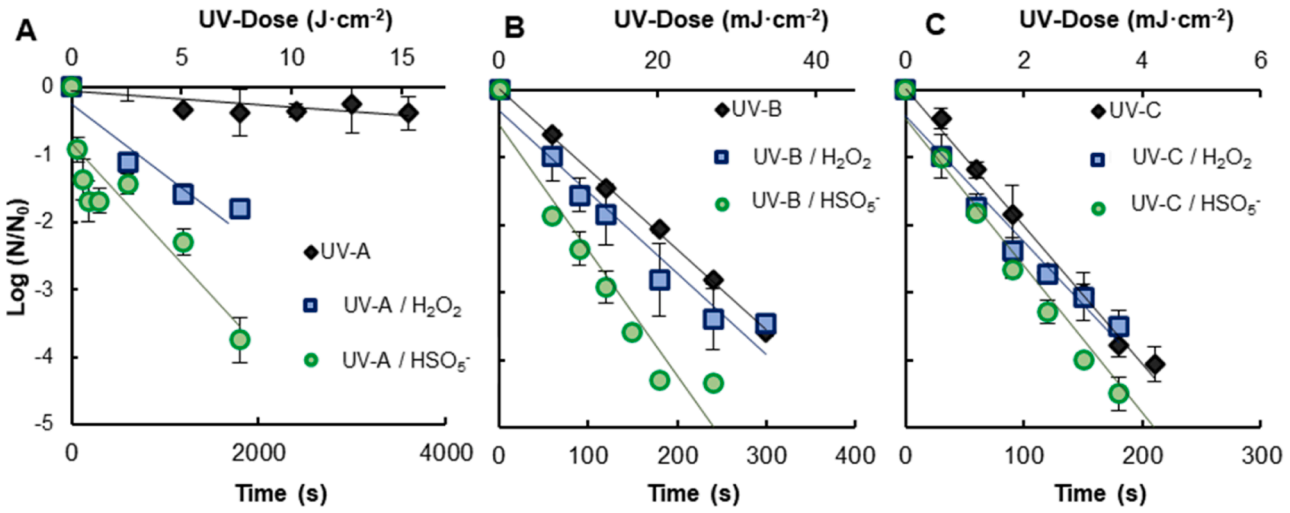

Fig. 2. Inactivation profiles of *V. alginolyticus* under UV/H_2O_2 ([H_2O_2] =10 mg·L^{-1}) or UV/HSO_5^- ([HSO_5^-]=2.5 mg·L^{-1}) processes at different wavelengths**: A.** UV-A (λ_{max} = 365 nm); **B.** UV-B (λ_{max} = 300 nm) or **C.** UV-C (λ_{max} = 275 nm). Symbols represent the mean of experimental points, and lines show a fit by Log-lineal model.

Supplementary Material, Text S2, Figs. S1, and S2. Once the effect of single treatments (*i.e.,* UV radiation (Table 1) and reagent effect (Text S2, Fig. S1)) were quantified, the combination of UV radiation in different emission ranges together with H_2O_2 or HSO_5^- were tested. Results in the form of inactivation profiles are depicted in Fig. 2.

For each of the different cases under study, it is observed that there is an improvement in the disinfection process when either H_2O_2 or HSO_5^- are applied in combination with the UV. The specific kinetic rate constants are summarized in Fig. 3, and they are also explicitly reported in Table 1. For the three UV emission wavelengths, the improvements are more noticeable with the use of HSO_5^- than with the use of H_2O_2 (Figs. 2 and 3) that is most perceptible in the UV-A range, followed by the UV-B, and then the UV-C. In fact, significant differences (comparing the slopes obtained in the inactivation curves) were obtained when comparing the

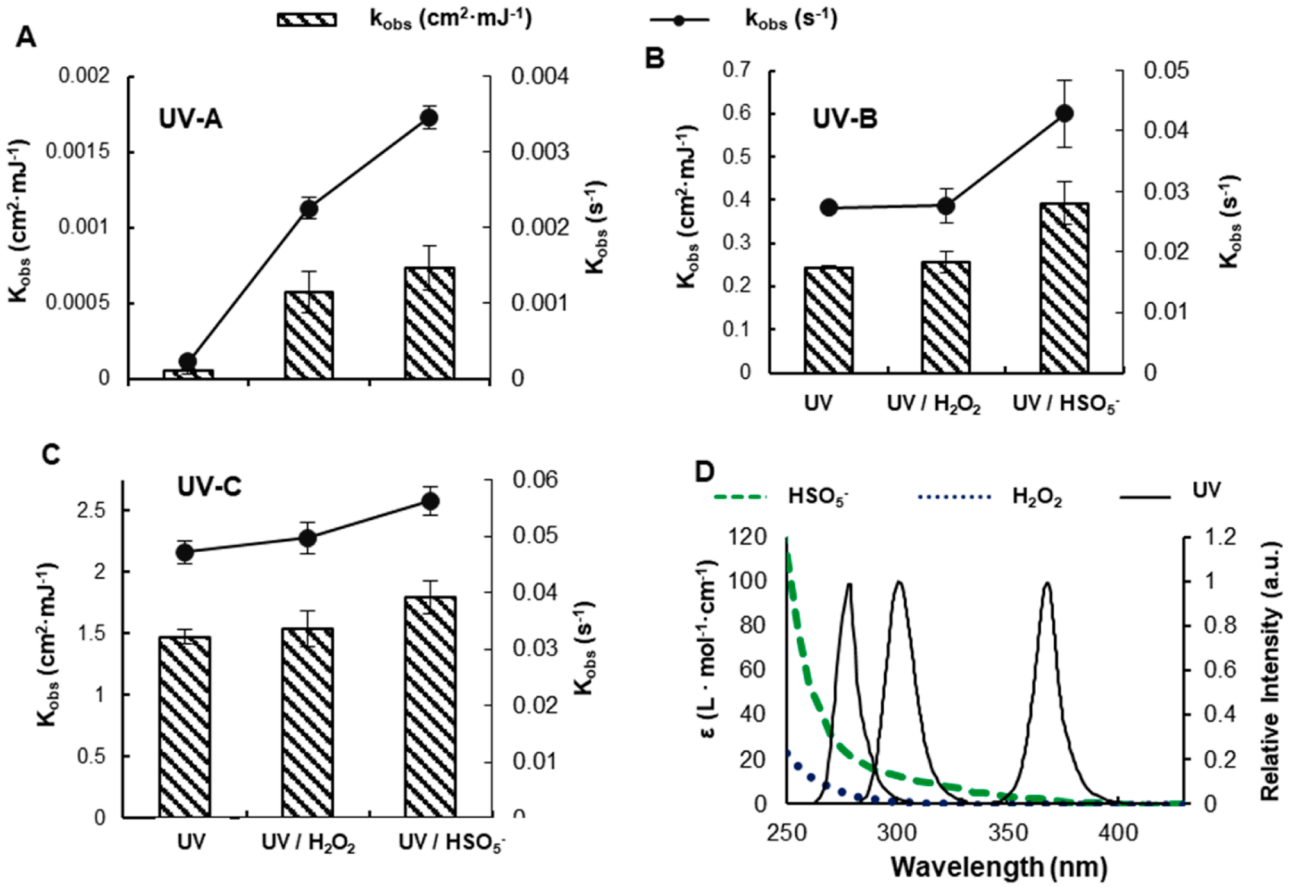

Fig. 3. Kinetic rate constant, k_{obs} (± S.E.), in terms of UV-Dose ($cm^2 \cdot mJ^{-1}$) and time (s^{-1}) for the different inactivation process UV/H_2O_2 ([H_2O_2] =10 mg·L^{-1}) or UV/HSO_5^- ([HSO_5^-]=2.50 mg·L^{-1}). **A.** UV-A (λ_{max} = 365 nm); **B.** UV-B (λ_{max} = 300 nm) or **C.** UV-C (λ_{max} = 275 nm). **D.** Molar absorption coefficient for H_2O_2 and HSO_5^- and emission spectra of each LED (UV-A, UV-B and UV-C).

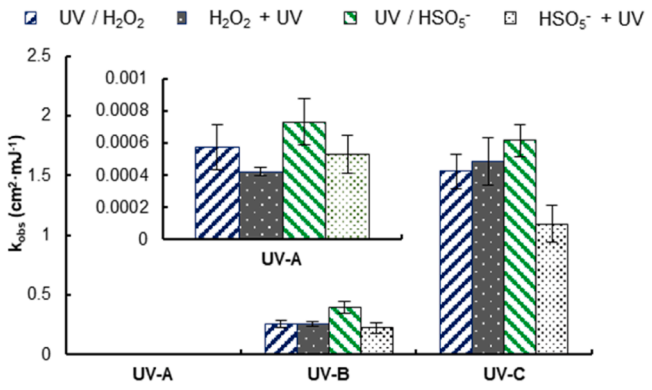

Fig. 4. Kinetic rate constant, k_{obs} (± S.E.), in terms of UV-Dose ($cm^2 \cdot mJ^{-1}$) and time (s^{-1}) for the different inactivation processes applied in a simultaneous (UV/H_2O_2 or UV/HSO_5^-) or sequential mode (H_2O_2 + UV or HSO_5^- + UV).

combined with the single irradiation process for UV-A/H_2O_2 or UV-A/HSO_5^-, UV-B/HSO_5^-, and UV-C/HSO_5^- (p value < 0.01). However, for UV-B/H_2O_2 (p value = 0.0583) and UV-C/H_2O_2 (p value = 0.3371), no significant differences were determined regarding the single irradiation process. H_2O_2 consumption rate increased from UV-C to UV-A ranges with remaining H_2O_2 concentrations of 7.45 mg $H_2O_2 \cdot L^{-1}$ (UV-A), 8.83 mg $H_2O_2 \cdot L^{-1}$ (UV-B), and 9.03 mg $H_2O_2 \cdot L^{-1}$ (UV-C). The detailed H_2O_2 consumption profiles are shown in Fig. S2.

Related to the UV-Dose, the results that were obtained suggest that it can be reduced down to 91.9% and 95.9% (UV-A), 18.1% and 52.6% (UV-B), or 20.7% and 33.9% (UV-C) for H_2O_2 and HSO_5^-, respectively. In addition, there was clearly a synergistic effect in the UV-A and UV-B range (Fig S4). This confirms that the improvement on combined processes is clearly evidenced at longer wavelengths, i.e., UV-A > UV-B > UV-C.

The increase in the efficiency of the disinfection process can be related to the formation of reactive oxygen species (ROS) in the extracellular environment. The photocleavage of H_2O_2 or HSO_5^- may depend on the wavelength applied. Thus, the photolysis of H_2O_2 or HSO_5^- will most likely occur when there is an overlap between the emission and absorbance spectra of the oxidizing agents (Fig. 3D). As can be seen in Fig. 3D, the molar absorption coefficient of HSO_5^- is higher than H_2O_2. In addition, HSO_5^- reaches the UV-A emission spectra which is contrary to the H_2O_2 that clearly extends to the UV-C and slightly reaches the UV-B spectrum. Accordingly, the generation of reactive species because of the photolysis of H_2O_2 is highly probable under the UV-C radiation and, to some extent, under the UV-B radiation. Meanwhile, the high molar absorption coefficient of HSO_5^- makes the photolysis of this compound possible under the UV-A, UV-B, and UV-C radiation.

When there is no overlapping of the emission and absorption spectra, the probable pathway of cell damage that is observed can be related to an intracellular effect. Section 3.1 Irradiation can inflict damage on genetic material but also on key ROS controlling enzymes, depending on the emission wavelength (Giannakis et al., 2016; Pousty et al., 2021; Santos et al., 2013). Additionally, the presence of H_2O_2 or HSO_5^- in the extracellular environment can lead to an accumulation of it in the cell (Berruti et al., 2021; Feng et al., 2020). As a result, the combination of UV and H_2O_2 or HSO_5^- can result in a series of intracellular processes such as Fenton (-like) reactions that would eventually inactivate the cells (Berruti et al., 2021; Feng et al., 2020; Giannakis et al., 2016). According to the results, intracellular processes might gain importance in the range of the UV-A, followed by the UV-B and, to a lesser extent, with UV-C radiation. This is in agreement with the H_2O_2 consumption rates that were obtained (Fig. S2).

Nonetheless, it is important to note that the high UV sensitivity of *V. alginolyticus* implies low UV exposure times with the subsequent low UV-Doses applied under the UV-C or UV-B exposures. This makes it difficult to effectively quantify the disinfection enhancement produced from combined UV/H_2O_2 or UV/HSO_5^-. Meanwhile, the longer exposure times of UV-A clearly permit the observation of disinfection enhancement from the photochemical processes.

3.2.2. H_2O_2 + UV and HSO_5^- + UV: sequential approach

At this point, experimentation was carried out in order to address the effects of combined processes but following a different strategy. The reagents were sequentially applied (H_2O_2 or HSO_5^- followed by UV) for providing enough time for H_2O_2 or HSO_5^- to penetrate the cell to initiate the intracellular oxidation. Thus, the addition of the reagent can be considered as pretreatment with UV irradiation as the secondary disinfectant.

Similar to that in the previous sections, inactivation profiles were obtained, and kinetic rate constants based on a linear inactivation model were determined. Thus, k_{obs} was represented in terms of UV-Dose ($cm^2 \cdot mJ^{-1}$) in Fig. 4. The specific inactivation profiles were represented in Fig. S5. Inactivation during the 30 min of darkness was 0.48 ± 0.17 LRV (H_2O_2) and 0.52 ± 0.22 LRV (HSO_5^-).

According to the values of inactivation rate constants, slight differences can be observed according to the oxidizing agent (H_2O_2 or HSO_5^-) and the irradiation wavelength. In the case of H_2O_2, the inactivation constant between the simultaneous and sequential process (i) decreases in the UV-A photo-assisted process, (ii) remains similar under the UV-B irradiation, and (iii) slightly increases under UV-C light. The consumption of H_2O_2 in the first 30 min of darkness was quantified as 26.7% (Fig. S6). This may be due to the inherent compounds at the bulk but also to the bacterial activity that is able to consume H_2O_2 but only minimally effects the survival of the microorganisms because of the scavenging action of the cell's enzymes, such as superoxide dismutase or catalases (Feng et al., 2020; Pedersen et al., 2019). The subsequent irradiation does not produce any enhancement in the case of the UV-A or UV-B ranges thus indicating that the possible previous diffusion of H_2O_2 into the cell apparently did not produce extra damage. However, the slight enhancement in the UV-C region (increase of 4.9% the k_{obs}) can be ascertained from the severe damages that single UV-C causes at low UV-Doses. At the same time, the photolysis of H_2O_2 can also be produced as previously discussed in Section 3.2.1. In fact, higher H_2O_2 consumption rates have been observed under UV-C exposure (Fig. S6). Similar results were obtained using *Bacillus subtilis* spores (Zhang et al., 2014).

On the other hand, in the case of HSO_5^-, the inactivation constant that was obtained always decreased under sequential processes in comparison with the simultaneous strategy (Fig. 4). These results can be related to the low concentrations of HSO_5^- used in the present study and their unstable nature. Therefore, a lower reagent amount will be available to interact with photons after 30 min. Consequently, the oxidative damage caused by the HSO_5^- itself does not result in a synergy if irradiation is applied after a certain amount of time.

Another strategy that could enhance disinfection would be the sequential application of a UV + oxidizing agent. In this regard, the damage caused by UV irradiation in any of its emission ranges would damage key cell components and subsequently facilitate the action of oxidizing agents to accelerate disinfection (Giannakis et al., 2022; Zhang et al., 2014). Some promising results were reported by sequentially combining single irradiation (UV-A + UV-C) (Xiao et al., 2018) or UV-C + H_2O_2 (Zhang et al., 2014), thus, future studies in this regard would be recommended to comprehensively assess this treatment strategy.

3.3. Regrowth after treatment

Due to the capacity of dark repair that some microorganisms have, regrowth can occasionally result from either surviving bacteria after inactivation together with reactivation or repair processes. Thus, the regrowth capability after treatment was evaluated for each photo-

chemical process of saving samples in the dark for 24 h.

The regrowth percentage is summarized in Table 1. According to the results, this occurs in each of the single irradiation tests (UV alone). Although, with lower regrowth percentages than UV alone, certain regrowth is observed in HSO_5^-based processes with either the UV-A or UV-B but is minor for UV-C. However, in the process combined with H_2O_2, a negligible regrowth is obtained for all tests.

The single irradiation processes that were tested are based on the exposure of *V. alginolyticus* at different UV wavelengths that vary in the bactericidal mode of action. The cell damage obtained from the UV-C region is mainly at the genome level while further cell components can be damaged as a result of UV-B or UV-A exposures. At the same time, the most germicidal wavelength is within the UV-C range, as confirmed by the inactivation profiles (Fig. 2, Table 1). Thus, the regrowth capability is directly related to the inactivation efficiency, obtaining the lowest regrowth percentages in samples exposed to the UV-C followed by those exposed to the UV-B.

In the combined UV/H_2O_2 process, the regrowth capability is prevented in all cases which indicates that the level of cellular aggressions is apparently high in this combined treatment. It can be a result of the severe damage produced in the cell due to hydroxyl radicals generated from the H_2O_2 photolysis (in the UV-C range) but also other intracellular processes that might take importance in the UV-A or UV-B processes. Moreover, the residual H_2O_2 (Fig. S2) can increase the accumulation rate in the cell and cause a growth defect.

Finally, for the combined UV/HSO_5^- process, regrowth is not avoided in 24 h in exposures to the UV-A and UV-B ranges; it is negligible in the case of the UV-C exposures. It highlights that UV/HSO_5^-, although sufficient to accelerate disinfection, does not seem to be sufficient to prevent subsequent regrowth.

3.4. Electrical energy per order (EE/O) values

To obtain a final overview of the different processes tested in the present study, the electrical energy per order values, EE/O (kWh·m^{-3}), were estimated and represented in Fig. 5. Following the same trends obtained in previous sections, the EE/O values decrease according to single UV processes > UV/H_2O_2 > UV/ HSO_5^- as they are directly related to the inactivation constant.

For single UV methods, the obtained EE/O values are 67.55, 0.38, and 0.04 kWh·m^{-3} for UV-A, UV-B, and UV-C, respectively. The combination with H_2O_2 results in an EE/O decrease of 96.80% (UV-A), 18.00% (UV-B), and 0.04% (UV-C) whereas the application of HSO_5^- implies an EE/O reduction of 97.50% (UV-A), 46.50% (UV-B), and 0.17% (UV-C).

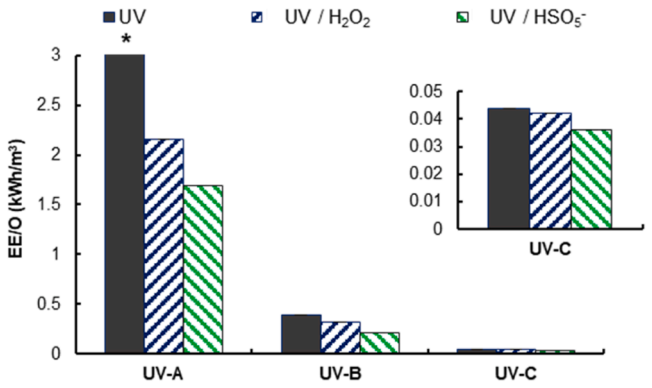

Fig. 5. EE/O (kWh·m^{-3} per order of log reduction) values obtained for the different inactivation processes UV/H_2O_2 ([H_2O_2] =10.0 mg·L^{-1}) or UV/HSO_5^- ([HSO_5^-]=2.5 mg·L^{-1}) and according to various emission wavelengths: UV-A (λ_{max} = 365 nm), UV-B (λ_{max} = 300 nm) or UV-C (λ_{max} = 275 nm). * For single UV-A process, the EE/O value obtained corresponds to 67.55 kWh·m^{-3}.

According to Miklos et al., 2018, those processes with EE/O < 1 kWh·m^{-3} may represent a realistic range for full-scale application. In this scenario, the UV-B or UV-C based processes present potential for their further study at larger scales. The UV-A process, although showing promising results from the enhancement with a combination with H_2O_2 or HSO_5^-, still presents values above 1 kWh·m^{-3}.

In any case, the estimated EE/O values presented in this study show promising potential for the application of UV-LEDs even in the range with those obtained with low and medium pressure mercury lamps (Miklos et al., 2018). Nonetheless, there is still a wide range for improvement, primarily due to the still low Wall-Plug Efficiency of LEDs.

4. Conclusions

In the present study, the efficacy of the disinfection of the marine pathogen *V. alginolyticus* is addressed by means of different UV-LED photochemical processes (with the use of H_2O_2 or HSO_5^-) that are distinguished according to the emission wavelengths of UV-A (λ_{max} = 365 nm), UV-B (λ_{max} = 300 nm), or UV-C (λ_{max} = 275 nm). Thus, the optimization of the UV-Dose and the wavelength effect for specific marine water disinfection is emphasized.

The disinfection efficacy based on the inactivation rate constants that were calculated is inversely proportional to the wavelength that is used, so that higher disinfection efficiency is achieved with shorter wavelengths: UV-A < UV-B < UV-C. *V. alginolyticus* presents high sensitivity to the UV-C and UV-B radiation with obtained values of 1.60 mJ·cm^{-2} and 9.50 mJ·cm^{-2} per LRV, respectively. Single UV-A irradiation does not produce observable inactivation (0.39 LRV at 18.1 J·cm^{-2}).

The three wavelengths tested exhibited a synergistic effect for both photochemical processes (UV/H_2O_2 and UV/HSO_5^-). Nonetheless, the major inactivation rate constants were for UV/HSO_5^- in front of UV/H_2O_2 process. Additionally, disinfection enhancement was more evident at longer wavelengths (UV-A > UV-B > UV-C), which suggests that intracellular processes might be important in the UV-A range, followed by UV-B irradiation and, to a lesser extent, UV-C radiation. It is also important to note the higher UV sensitivity of *V. alginolyticus* and, thus, the lower UV doses applied in the UV-B and UV-C regions. On the other hand, application in the sequential mode (HSO_5^- or H_2O_2 + UV) provided negligible results in the inactivation of *V. alginolyticus* when compared with the simultaneous mode.

Bacterial regrowth was only avoided after 24 h with the use of H_2O_2. Thus, although with slightly lower inactivation rates compared to UV/HSO_5^-, the level of cellular aggression was apparently higher in the UV/H_2O_2 process. Finally, both photochemical systems present promising EEO values, especially when applied with LEDs emitting in the UV-B or UV-C region, for which EEO < 1 kWh·m^{-3} was obtained.

Declaration of Competing Interest

The authors declare that they have no known competing financial interests or personal relationships that could have appeared to influence the work reported in this paper.

Data availability

Data will be made available on request.

Acknowledgments

This work was co-funded by the 2014–2020 ERDF Operational Programme and by the Department of Economy, Knowledge, Business and University of the Regional Government of Andalusia (Spain). Project Ref.: FEDER-UCA18–108023. This work is part of the project TED2021–130994B-C31 and Grant IJC2020–042741-I funded by MCIN/

AEI/10.13039/501100011033 and by the European Union NextGenerationEU/PRTR. M. Tierno-Galán developed his MSc thesis within the framework of this study in the "Máster Universitario en Gestión Integral del Agua" of University of Cádiz.

Supplementary materials

Supplementary material associated with this article can be found, in the online version, at doi:10.1016/j.watres.2023.119686.

References

Aguilar, S., Rosado, D., Moreno-Andrés, J., Cartuche, L., Cruz, D., Acevedo-Merino, A., Nebot, E., 2018. Inactivation of a wild isolated Klebsiella pneumoniae by photochemical processes: UV-C, UV-C/H2O2and UV-C/H2O2/Fe3+. Catal. Today 313, 94–99. https://doi.org/10.1016/j.cattod.2017.10.043.

Baker-Austin, C., Trinanes, J., Gonzalez-Escalona, N., Martinez-Urtaza, J., 2017. Non-cholera vibrios: the microbial barometer of climate change. Trends Microbiol. 25, 76–84. https://doi.org/10.1016/j.tim.2016.09.008.

Beck, S.E., Ryu, H., Boczek, L.A., Cashdollar, J.L., Jeanis, K.M., Rosenblum, J.S., Lawal, O.R., Linden, K.G., 2017. Evaluating UV-C LED disinfection performance and investigating potential dual-wavelength synergy. Water Res. 109, 207–216. https://doi.org/10.1016/J.WATRES.2016.11.024.

Belkin, S., Colwell, R.R., 2005. Oceans and Health: Pathogens in the Marine Environment. Springer.

Bellés-Garulera, J., Vila, M., Borrull, E., Riobó, P., Franco, J.M., Sala, M.M., 2016. Variability of planktonic and epiphytic vibrios in a coastal environment affected by Ostreopsisblooms. Sci. Mar. 80, 97–106. https://doi.org/10.3989/SCIMAR.04405.01A.

Berruti, I., Nahim-Granados, S., Abeledo-Lameiro, M.J., Oller, I., Polo-López, M.I., 2022. Recent advances in solar photochemical processes for water and wastewater disinfection. Chem. Eng. J. Adv. 10, 100248 https://doi.org/10.1016/J.CEJA.2022.100248.

Berruti, I., Oller, I., Polo-López, M.I., 2021. Direct oxidation of peroxymonosulfate under natural solar radiation: accelerating the simultaneous removal of organic contaminants and pathogens from water. Chemosphere 279, 130555. https://doi.org/10.1016/j.chemosphere.2021.130555.

Bolton, J.R., Cotton, C.A., 2008. The Ultraviolet Disinfection Handbook. American Water Works Association, Denver.

Bolton, J.R., Linden, K.G., 2003. Standardization of methods for fluence (UV Dose) determination in bench-scale UV experiments. J. Environ. Eng. 129, 209–215. https://doi.org/10.1061/(ASCE)0733-9372(2003)129:3(209).

Chen, J., Loeb, S., Kim, J.-.H., 2017. LED revolution: fundamentals and prospects for UV disinfection applications. Environ. Sci. Water Res. Technol. 3, 188–202. https://doi.org/10.1039/C6EW00241B.

Dewil, R., Mantzavinos, D., Poulios, I., Rodrigo, M.A., 2017. New perspectives for advanced oxidation processes. J. Environ. Manage. 195, 93–99. https://doi.org/10.1016/J.JENVMAN.2017.04.010.

Feng, L., Peillex-Delphe, C., Lü, C., Wang, D., Giannakis, S., Pulgarin, C., 2020. Employing bacterial mutations for the elucidation of photo-Fenton disinfection: focus on the intracellular and extracellular inactivation mechanisms induced by UVA and H2O2. Water Res. 182, 116049 https://doi.org/10.1016/j.watres.2020.116049.

Geeraerd, A.H., Valdramidis, V.P., Van Impe, J.F., 2005. GInaFiT, a freeware tool to assess non-log-linear microbial survivor curves. Int. J. Food Microbiol. 102, 95–105. https://doi.org/10.1016/j.ijfoodmicro.2004.11.038.

Giannakis, S., Gupta, A., Pulgarin, C., Imlay, J., 2022. Identifying the mediators of intracellular E. coli inactivation under UVA light: the (photo)Fenton process and singlet oxygen. Water Res. 118740 https://doi.org/10.1016/J.WATRES.2022.118740.

Giannakis, S., Merino Gamo, A.I., Darakas, E., Escalas-Cañellas, A., Pulgarin, C., 2014. Monitoring the post-irradiation E. coli survival patterns in environmental water matrices: implications in handling solar disinfected wastewater. Chem. Eng. J. 253, 366–376. https://doi.org/10.1016/j.cej.2014.05.092.

Giannakis, S., Polo López, M.I., Spuhler, D., Sánchez Pérez, J.A., Fernández Ibáñez, P., Pulgarin, C., 2016. Solar disinfection is an augmentable, in situ-generated photo-Fenton reaction—Part 1: a review of the mechanisms and the fundamental aspects of the process. Appl. Catal. B Environ. 199, 199–223. https://doi.org/10.1016/j.apcatb.2016.06.009.

Guerra-Rodríguez, S., Rodríguez, E., Moreno-Andrés, J., Rodríguez-Chueca, J., 2022. Effect of the water matrix and reactor configuration on Enterococcus sp. inactivation by UV-A activated PMS or H2O2. J. Water Process Eng. 47, 102740 https://doi.org/10.1016/J.JWPE.2022.102740.

Hess-Erga, O.-K., Moreno-Andrés, J., Enger, Ø., Vadstein, O., 2019. Microorganisms in ballast water: disinfection, community dynamics, and implications for management. Sci. Total Environ. 657, 704–716. https://doi.org/10.1016/J.SCITOTENV.2018.12.004.

Hess-Erga, O.K., Blomvågnes-Bakke, B., Vadstein, O., 2010. Recolonization by heterotrophic bacteria after UV irradiation or ozonation of seawater; a simulation of ballast water treatment. Water Res. 44, 5439–5449. https://doi.org/10.1016/j.watres.2010.06.059.

IMO, 2004. International Convention for the Control and Management of Ships' Ballast Water and Sediments. BWM/CONF/36.

Jeon, I., Ryberg, E.C., Alvarez, P.J.J., Kim, J.-.H., 2022. Technology assessment of solar disinfection for drinking water treatment. Nat. Sustain. 2022, 1–8. https://doi.org/10.1038/s41893-022-00915-7.

Jo, W.K., Tayade, R.J., 2014. New generation energy-efficient light source for photocatalysis: LEDs for environmental applications. Ind. Eng. Chem. Res. 53, 2073–2084. https://doi.org/10.1021/ie404176g.

Khandeparker, L., Kuchi, N., Desai, D.V., Anil, A.C., 2020. Changes in the ballast water tank bacterial community during a trans-sea voyage: elucidation through next generation DNA sequencing. J. Environ. Manage. 273, 111018 https://doi.org/10.1016/j.jenvman.2020.111018.

Levchuk, I., Homola, T., Moreno-Andrés, J., Rueda-márquez, J.J., Dzik, P., Ángel, M., Sillanpää, M., Manzano, M.A., Vahala, R., 2019. Solar photocatalytic disinfection using ink-jet printed composite TiO2/SiO2 thin films on flexible substrate : applicability to drinking and marine water. Sol. Energy 191, 518–529. https://doi.org/10.1016/j.solener.2019.09.038.

Li, X., Cai, M., Wang, L., Niu, F., Yang, D., Zhang, G., 2019. Evaluation survey of microbial disinfection methods in UV-LED water treatment systems. Sci. Total Environ. 659, 1415–1427. https://doi.org/10.1016/J.SCITOTENV.2018.12.344.

Lindenauer, K.G., Darby, J.L., 1994. Ultraviolet disinfection of wastewater: effect of dose on subsequent photoreactivation. Water Res. 28, 805–817. https://doi.org/10.1016/0043-1354(94)90087-6.

Martín-Sómer, M., Molina-Ramírez, M.D., Perez-Araujo, M.L., Van Grieken, R., Marug, J., 2023. Comparing the efficiency of solar water treatment : photovoltaic-LED vs compound parabolic collector photoreactors. J. Environ. Chem. Eng. 11, 109332 https://doi.org/10.1016/j.jece.2023.109332.

Martín-Sómer, M., Vega, B., Pablos, C., van Grieken, R., Marugán, J., 2018. Wavelength dependence of the efficiency of photocatalytic processes for water treatment. Appl. Catal. B Environ. 221, 258–265. https://doi.org/10.1016/J.APCATB.2017.09.032.

Miklos, D.B., Remy, C., Jekel, M., Linden, K.G., Drewes, J.E., Hübner, U., 2018. Evaluation of advanced oxidation processes for water and wastewater treatment – A critical review. Water Res. 139, 118–131. https://doi.org/10.1016/j.watres.2018.03.042.

Moreno-Andrés, J., Acevedo-Merino, A., Nebot, E., 2018. Study of marine bacteria inactivation by photochemical processes: disinfection kinetics and growth modeling after treatment. Environ. Sci. Pollut. Res. 25, 27693–27703. https://doi.org/10.1007/s11356-017-1185-6.

Moreno-Andrés, J., Farinango, G., Romero-Martínez, L., Acevedo-Merino, A., Nebot, E., 2019. Application of persulfate salts for enhancing UV disinfection in marine waters. Water Res. 163, 114866 https://doi.org/10.1016/J.WATRES.2019.114866.

Moreno-Andrés, J., Morillo-Ponce, J., Ibáñez-López, M.E., Acevedo-Merino, A., García-Morales, J.L., 2020a. Disinfection enhancement of single ozonation by combination with peroxymonosulfate salt. J. Environ. Chem. Eng. 8, 104335 https://doi.org/10.1016/j.jece.2020.104335.

Moreno-Andrés, J., Romero-Martínez, L., Acevedo-Merino, A., Nebot, E., 2017. UV-based technologies for marine water disinfection and the application to ballast water: does salinity interfere with disinfection processes? Sci. Total Environ. 581–582, 144–152. https://doi.org/10.1016/j.scitotenv.2016.12.077.

Moreno-Andrés, J., Romero-Martínez, L., Acevedo-Merino, A., Nebot, E., 2016. Determining disinfection efficiency on E. faecalis in saltwater by photolysis of H2O2: implications for ballast water treatment. Chem. Eng. J. 283, 1339–1348. https://doi.org/10.1016/j.cej.2015.08.079.

Moreno-Andrés, J., Rueda-Márquez, J.J., Homola, T., Vielma, J., Moríñigo, M.Á., Mikola, A., Sillanpää, M., Acevedo-Merino, A., Nebot, E., Levchuk, I., 2020b. A comparison of photolytic, photochemical and photocatalytic processes for disinfection of recirculation aquaculture systems (RAS) streams. Water Res. 181, 115928 https://doi.org/10.1016/j.watres.2020.115928.

Nakahashi, M., Mawatari, K., Hirata, A., Maetani, M., Shimohata, T., Uebanso, T., Hamada, Y., Akutagawa, M., Kinouchi, Y., Takahashi, A., 2014. Simultaneous irradiation with different wavelengths of ultraviolet light has synergistic bactericidal effect on vibrio parahaemolyticus. Photochem. Photobiol. 90, 1397–1403. https://doi.org/10.1111/php.12309.

Ng, C., Goh, S.G., Saeidi, N., Gerhard, W.A., Gunsch, C.K., Gin, K.Y.H., 2018. Occurrence of Vibrio species, beta-lactam resistant Vibrio species, and indicator bacteria in ballast and port waters of a tropical harbor. Sci. Total Environ. 610–611, 651–656. https://doi.org/10.1016/j.scitotenv.2017.08.099.

Nyangaresi, P.O., Qin, Y., Chen, G., Zhang, B., Lu, Y., Shen, L., 2018. Effects of single and combined UV-LEDs on inactivation and subsequent reactivation of E. coli in water disinfection. Water Res. 147, 331–341. https://doi.org/10.1016/j.watres.2018.10.014.

Oguma, K., Rattanakul, S., Masaike, M., 2019. Inactivation of health-related microorganisms in water using UV light-emitting diodes. Water Supply 19, 1507–1514. https://doi.org/10.2166/WS.2019.022.

Pedersen, L.-F., Rojas-Tirado, P., Arvin, E., Pedersen, P.B., 2019. Assessment of microbial activity in water based on hydrogen peroxide decomposition rates. Aquac. Eng. 85, 9–14. https://doi.org/10.1016/J.AQUAENG.2019.01.001.

Pesqueira, J.F.J.R., Marugán, J., Pereira, M.F.R., Silva, A.M.T., 2022. Selecting the most environmentally friendly oxidant for UVC degradation of micropollutants in urban wastewater by assessing life cycle impacts: hydrogen peroxide, peroxymonosulfate or persulfate? Sci. Total Environ. 808, 152050 https://doi.org/10.1016/J.SCITOTENV.2021.152050.

Porcar-Santos, O., Cruz-Alcalde, A., López-Vinent, N., Zanganas, D., Sans, C., 2020. Photocatalytic degradation of sulfamethoxazole using TiO2 in simulated seawater: evidence for direct formation of reactive halogen species and halogenated by-products. Sci. Total Environ. 736, 139605 https://doi.org/10.1016/j.scitotenv.2020.139605.

Pousty, D., Hofmann, R., Gerchman, Y., Mamane, H., 2021. Wavelength-dependent time–dose reciprocity and stress mechanism for UV-LED disinfection of Escherichia coli. J. Photochem. Photobiol. B Biol. 217, 112129 https://doi.org/10.1016/J.JPHOTOBIOL.2021.112129.

Qi, W., Zhu, S., Shitu, A., Ye, Z., Liu, D., 2020. Low concentration peroxymonosulfate and UVA-LED combination for E. coli inactivation and wastewater disinfection from recirculating aquaculture systems. J. Water Process Eng. 36, 101362 https://doi.org/10.1016/j.jwpe.2020.101362.

Rattanakul, S., Oguma, K., 2018. Inactivation kinetics and efficiencies of UV-LEDs against Pseudomonas aeruginosa, Legionella pneumophila, and surrogate microorganisms. Water Res. 130, 31–37. https://doi.org/10.1016/J.WATRES.2017.11.047.

Reen, F.J., Almagro-Moreno, S., Ussery, D., Boyd, E.F., 2006. The genomic code: inferring Vibrionaceae niche specialization. Nat. Rev. Microbiol. 4, 697–704. https://doi.org/10.1038/nrmicro1476.

Rodríguez-Chueca, J., Giannakis, S., Marjanovic, M., Kohantorabi, M., Gholami, M.R., Grandjean, D., de Alencastro, L.F., Pulgarín, C., 2019. Solar-assisted bacterial disinfection and removal of contaminants of emerging concern by Fe2+-activated HSO5- vs. S2O82- in drinking water. Appl. Catal. B Environ. 248, 62–72. https://doi.org/10.1016/J.APCATB.2019.02.018.

Romero-Martínez, L., Moreno-Andrés, J., Acevedo-Merino, A., Nebot, E., 2022. Development of a geometrical model for the determination of the average intensity in a flow-through UV-LED reactor and validation with biodosimetry and actinometry. J. Water Process Eng. 49, 103137 https://doi.org/10.1016/J.JWPE.2022.103137.

Rubio, D., Casanueva, J.F., Nebot, E., 2015. Assessment of the antifouling effect of five different treatment strategies on a seawater cooling system. Appl. Therm. Eng. 85, 124–134. https://doi.org/10.1016/j.applthermaleng.2015.03.080.

Santos, A.L., Oliveira, V., Baptista, I., Henriques, I., Gomes, N.C.M., Almeida, A., Correia, A., Cunha, Â., 2013. Wavelength dependence of biological damage induced by UV radiation on bacteria. Arch. Microbiol. 195, 63–74. https://doi.org/10.1007/s00203-012-0847-5.

Sharpless, C.M., Linden, K.G., 2005. Interpreting collimated beam ultraviolet photolysis rate data in terms of electrical efficiency of treatment. J. Environ. Eng. Sci. 4 https://doi.org/10.1139/s04-045.

Song, K., Mohseni, M., Taghipour, F., 2016. Application of ultraviolet light-emitting diodes (UV-LEDs) for water disinfection: a review. Water Res. 94, 341–349. https://doi.org/10.1016/j.watres.2016.03.003.

Song, K., Taghipour, F., Mohseni, M., 2019. Microorganisms inactivation by wavelength combinations of ultraviolet light-emitting diodes (UV-LEDs). Sci. Total Environ. 665, 1103–1110. https://doi.org/10.1016/J.SCITOTENV.2019.02.041.

Summerfelt, S.T., 2003. Ozonation and UV irradiation—An introduction and examples of current applications. Aquac. Eng. 28, 21–36. https://doi.org/10.1016/S0144-8609(02)00069-9.

Umar, M., Roddick, F., Fan, L., 2019. Moving from the traditional paradigm of pathogen inactivation to controlling antibiotic resistance in water - Role of ultraviolet irradiation. Sci. Total Environ. 662, 923–939. https://doi.org/10.1016/J.SCITOTENV.2019.01.289.

UNEP, 2019. Minamata Convention on Mercury 72. https://doi.org/www.mercuryconvention.org.

Wacławek, S., Grübel, K., Černík, M., 2015. Simple spectrophotometric determination of monopersulfate. Spectrochim. Acta - Part A Mol. Biomol. Spectrosc. 149, 928–933. https://doi.org/10.1016/j.saa.2015.05.029.

Wang, W., Xie, H., Li, G., Li, J., Wong, P.K., An, T., 2021. Visible light-induced marine bacterial inactivation in seawater by an *In Situ* photo-fenton system without additional oxidants: implications for ballast water sterilization. ACS EST Water. https://doi.org/10.1021/acsestwater.1c00048 acsestwater.1c00048.

Wennberg, A.C., Tryland, I., Østensvik, Ø., Secic, I., Monshaugen, M., Liltved, H., 2013. Effect of water treatment on the growth potential of Vibrio cholerae and Vibrio parahaemolyticus in seawater. Mar. Environ. Res. 83, 10–15. https://doi.org/10.1016/j.marenvres.2012.10.002.

Xiao, Y., Chu, X.N., He, M., Liu, X.C., Hu, J.Y., 2018. Impact of UVA pre-radiation on UVC disinfection performance: inactivation, repair and mechanism study. Water Res. 141, 279–288. https://doi.org/10.1016/j.watres.2018.05.021.

Zhang, Y., Wei, M., Huang, K., Yu, K., Liang, J., Wei, F., Huang, J., Yin, X., 2022. Inactivation of E. coli and Streptococcus agalactiae by UV/persulfate during marine aquaculture disinfection. Environ. Sci. Pollut. Res. 29, 45421–45434. https://doi.org/10.1007/s11356-022-19108-y.

Zhang, Yongji, Zhang, Yiqing, Zhou, L., Tan, C., 2014. Inactivation of bacillus subtilis spores using various combinations of ultraviolet treatment with addition of hydrogen peroxide. Photochem. Photobiol. 90, 609–614. https://doi.org/10.1111/php.12210.